Role of arm reaching movement kinematics in friction perception at initial contact with smooth surfaces

Afzal, Naqash; du Bois de Dunilac, Sophie; Loutit, Alastair J.; Shea, Helen O.; Ulloa, Pablo Martinez; Khamis, Heba; Vickery, Richard M.; Wiertlewski, Michaël; Redmond, Stephen J.; Birznieks, Ingvars

DOI
10.1113/JP286027

Publication date
2024

Document Version
Final published version

Published in
Journal of Physiology

Citation (APA)
Afzal, N., du Bois de Dunilac, S., Loutit, A. J., Shea, H. O., Ulloa, P. M., Khamis, H., Vickery, R. M., Wiertlewski, M., Redmond, S. J., & Birznieks, I. (2024). Role of arm reaching movement kinematics in friction perception at initial contact with smooth surfaces. *Journal of Physiology*, *602*(9), 2089-2106. https://doi.org/10.1113/JP286027

Important note
To cite this publication, please use the final published version (if applicable).
Please check the document version above.

The Journal of Physiology

Role of arm reaching movement kinematics in friction perception at initial contact with smooth surfaces

Naqash Afzal[1,2,3,4], Sophie du Bois de Dunilac[5], Alastair J. Loutit[1,2], Helen O. Shea[6], Pablo Martinez Ulloa[5], Heba Khamis[7], Richard M. Vickery[1,2,8], Michaël Wiertlewski[9], Stephen J. Redmond[5] and Ingvars Birznieks[1,2,8]

[1]*School of Biomedical Sciences, UNSW Sydney, Sydney, NSW, Australia*
[2]*Neuroscience Research Australia, Sydney, NSW, Australia*
[3]*Department of Mechanical Engineering, Khalifa University, Abu Dhabi, United Arab Emirates*
[4]*Center for Autonomous Robotic Systems, Khalifa University, Abu Dhabi, United Arab Emirates*
[5]*School of Electrical and Electronic Engineering, University College Dublin, Dublin, Ireland*
[6]*Department of Psychology, University of Limerick, Limerick, Ireland*
[7]*Graduate School of Biomedical Engineering, UNSW Sydney, Sydney, NSW, Australia*
[8]*Bionics and Biorobotics, Tyree Foundation Institute of Health Engineering, UNSW Sydney, Sydney, NSW, Australia*
[9]*Department of Cognitive Robotics, Delft University of Technology, Delft, The Netherlands*

Handling Editors: Richard Carson & Ross Pollock

The peer review history is available in the Supporting Information section of this article (https://doi.org/10.1113/JP286027#support-information-section).

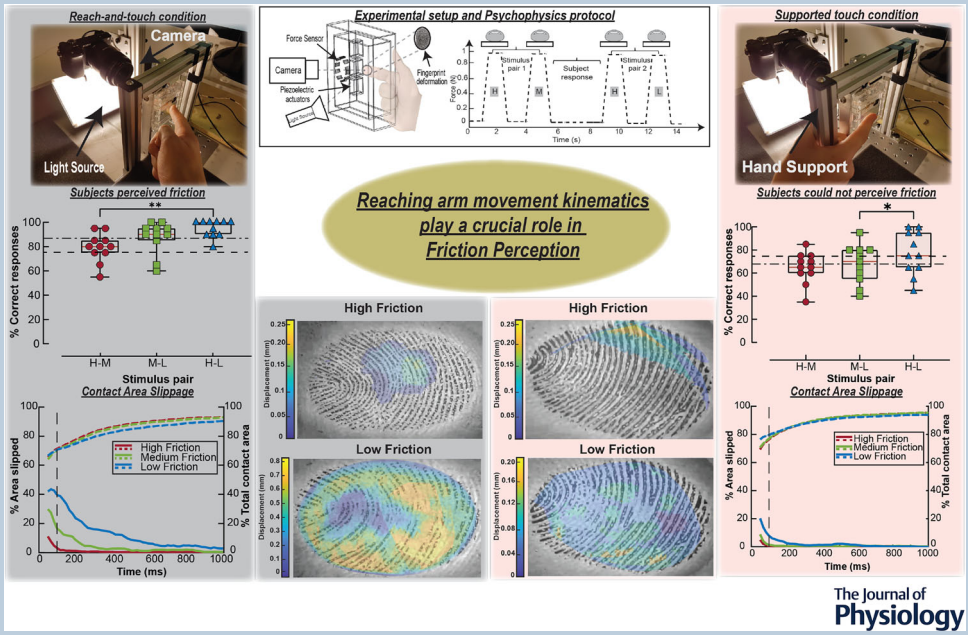

Abstract When manipulating objects, humans begin adjusting their grip force to friction within 100 ms of contact. During motor adaptation, subjects become aware of the slipperiness of touched surfaces. Previously, we have demonstrated that humans cannot perceive frictional differences when surfaces are brought in contact with an immobilised finger, but can do so when there is

This article was first published as a preprint. Afzal N, de Dunilac SdB, Loutit AJ, Shea HO, Martinez Ulloa P, Khamis H, Vickery RM, Wiertlewski M, Redmond SJ, Birznieks I. 2023. Role of finger movement kinematics in friction perception at initial contact with smooth surfaces. bioRxiv. https://doi.org/10.1101/2023.10.29.564644

DOI: 10.1113/JP286027

submillimeter lateral displacement or subjects actively make the contact movement. Similarly, in, we investigated how humans perceive friction in the absence of intentional exploratory sliding or rubbing movements, to mimic object manipulation interactions. We used a two-alternative forced-choice paradigm in which subjects had to reach and touch one surface followed by another, and then indicate which felt more slippery. Subjects correctly identified the more slippery surface in 87 ± 8% of cases (mean ± SD; $n = 12$). Biomechanical analysis of finger pad skin displacement patterns revealed the presence of tiny (<1 mm) localised slips, known to be sufficient to perceive frictional differences. We tested whether these skin movements arise as a result of natural hand reaching kinematics. The task was repeated with the introduction of a hand support, eliminating the hand reaching movement and minimising fingertip movement deviations from a straight path. As a result, our subjects' performance significantly declined (66 ± 12% correct, mean ± SD; $n = 12$), suggesting that unrestricted reaching movement kinematics and factors such as physiological tremor, play a crucial role in enhancing or enabling friction perception upon initial contact.

(Received 23 November 2023; accepted after revision 12 March 2024; first published online 28 March 2024)
Corresponding author N. Afzal: School of Biomedical Sciences, UNSW Sydney, Sydney, NSW 2031, Australia. Email: hafiz.afzal@ku.ac.ae

Abstract figure legend Reaching arm movement kinematics induces submillimeter range localised slips, which enables friction sensing when touching objects.

Key points

- More slippery objects require a stronger grip to prevent them from slipping out of hands.
- Grip force adjustments to friction driven by tactile sensory signals are largely automatic and do not necessitate cognitive involvement; nevertheless, some associated awareness of grip surface slipperiness under such sensory conditions is present and helps to select a safe and appropriate movement plan.
- When gripping an object, tactile receptors provide frictional information without intentional rubbing or sliding fingers over the surface. However, we have discovered that submillimeter range lateral displacement might be required to enhance or enable friction sensing.
- The present study provides evidence that such small lateral movements causing localised partial slips arise and are an inherent part of natural reaching movement kinematics.

Introduction

A safe grip between the fingertip skin and a surface can only be established if the applied grip force is sufficiently large to create a friction force that is equal to the load force developing tangential to the surface (Johansson & Westling, 1987). The motor control system achieves adequate grip force control by adjusting it to the frictional properties of the surface and skin (Johansson & Flanagan, 2009). When we hold objects such as tools in our hands, in addition to automatic motor adjustments, there is also a conscious sensory awareness of how slippery the gripped surface is and whether there is sufficient traction provided by the skin to perform the intended action safely. The sensory mechanisms enabling perception of surface slipperiness under the conditions commonly encountered

Naqash Afzal received his PhD from the University of New South Wales, Australia, under the prestigious Scientia PhD Scholarship Program with a distinction and Dean's Award for best PhD thesis. Dr Hafiz's research was conducted at leading laboratories in the field of haptics, tactile sensing and somatosensory research. During his postdoctoral training at the Neuroscience Research Australia in Sydney Australia, he broadened his research competence by investigating mechanisms and function of the autonomic nervous system for friction perception and dynamic force regulation during grasping and manipulating objects in humans. Currently, he is a postdoctoral researcher at the Khalifa University Abu Dhabi.

during object manipulation, without sliding or rubbing movements of the fingertips over the surface, are not well understood.

In previous studies, we investigated whether humans could perceive frictional differences between surfaces just by touching a surface without performing sliding movements (Khamis et al., 2021). Biomechanical investigations indicate that skin deformation patterns can efficiently reflect the frictional condition (Barrea et al., 2018; Delhaye et al., 2014, 2016; Johansson & Flanagan, 2009) and thus could be conveyed by tactile afferent responses (Khamis et al., 2014a, b). However, when surfaces were brought into contact with an immobilised finger (passive touch), subjects were unable to differentiate the slipperiness of either smooth or textured surfaces. We hypothesised that, because slipperiness perception in this context is pertinent to manipulation, an active movement might be required to enable sensory perception. Experiments in which subjects themselves actively contacted the surface (active touch) with a finger constrained to move along the normal of the contact surface demonstrated that a radial divergence pattern was sufficient to sense frictional differences; however, this ability depends on optimised contact kinetics and is most efficient when friction is low (Willemet et al., 2021). Further investigations using passive touch, where the object moves to contact the finger, revealed that active movement is not necessary to perceive frictional differences because a submillimeter range lateral movement as small as 0.2–0.5 mm of the surface relative to the affixed rigid nail–phalangeal bone complex is sufficient to perceive surface slipperiness, even with a larger coefficient of friction (Afzal et al., 2022). Overall, it has become evident that intentional exploratory sliding movements and gross slip are not required to perceive surface slipperiness. Variation in outcomes between experimental conditions indicates that the nervous system uses various types of cues and sources of sensory information, depending on availability. For example, with more slippery smooth surfaces, radially divergent skin deformation patterns might be most informative and sufficient to convey frictional information, especially when there is only small resultant tangential force developing and detection of the lateral slip over smooth surfaces is difficult (Willemet et al., 2021). By contrast, with surfaces in the higher friction range, which represent most often handled objects, the divergence is overall small and thus less informative. Slipperiness discrimination within this range instead may be more reliant on partial slip detection and skin stretch requiring presence of small lateral movements of the fingertip tangential to the surface.

Natural movements, when reaching and gripping objects, would rarely occur in perfectly straight path without the presence of subtle lateral back-and-forth deviations from the planned path originating from various sources, including physiological tremor and goal-directed movement correction. At the end point of reaching movement, this may translate into small lateral movement of the rigid nail–phalangeal bone complex relative to the object's surface, which creates stress and strain patterns resulting in a pattern of localised slips occurring within fingertip skin contact area. We hypothesise that natural movement kinematics producing minor lateral displacements could be the key to enabling us to evaluate the surface slipperiness when gripping and handling an object or tool.

In the present study, subjects evaluated similar frictional differences, as in our previous study (Khamis et al., 2021), in which subjects were unable to discriminate between two surfaces when using passive touch, but with subjects now asked to touch the surfaces themselves in a natural way. Using fingerprint image processing techniques, we evaluated the presence of partial slips linked to the ability of subjects to discriminate surface slipperiness. To confirm that reaching movement kinematics had a decisive role in the ability of subjects to evaluate slipperiness, we performed another experiment in which fingertip contact with a surface was made without an arm reaching movement, and we observed that, as a result, subjects' performance deteriorated significantly.

Methods

Ethical approval

The experimental protocols were approved by the Human Research Ethics Committee (approval number HC180109) at UNSW Sydney. The study conformed to the standards set by the *Declaration of Helsinki*, except for registration in a database. All the subjects provided written consent before the start of the experiment.

Subjects

Twelve healthy right-hand-dominant subjects (age 26.1 ± 6.2 years, mean ± SD; four female) participated in the experiment. All subjects in the study reported no history of neurological disorders and presented no clinical signs that would indicate altered skin sensitivity or motor function of the hand. Subjects cleaned their fingers with alcohol wipes before commencing the experimental protocol.

Friction modulation

An ultrasonic friction reduction device (Wiertlewski et al., 2016) was used to change the friction of a smooth

glass surface. The piezoelectric elements of the friction modulation device were driven by a waveform generator (DG 1022; RIGOL Technologies, Beijing, China) via a high-voltage amplifier (A-303; A.A. Lab Systems Ltd, Israel). Three levels of friction, high (H), medium (M) and low (L), were obtained by varying the driving voltage amplitude. MATLAB 2018a (MathWorks, Natick, MA, USA) was used to control the drive voltage amplitude of the friction reduction device via the analog output of a data acquisition unit (USB-6218; National Instruments, TX, USA). The friction reduction device was mounted on a custom-developed platform attached to a six-axis ATI Nano17 force-torque sensor (ATI Industrial Automation, NC, USA). The setup is illustrated in Fig. 1.

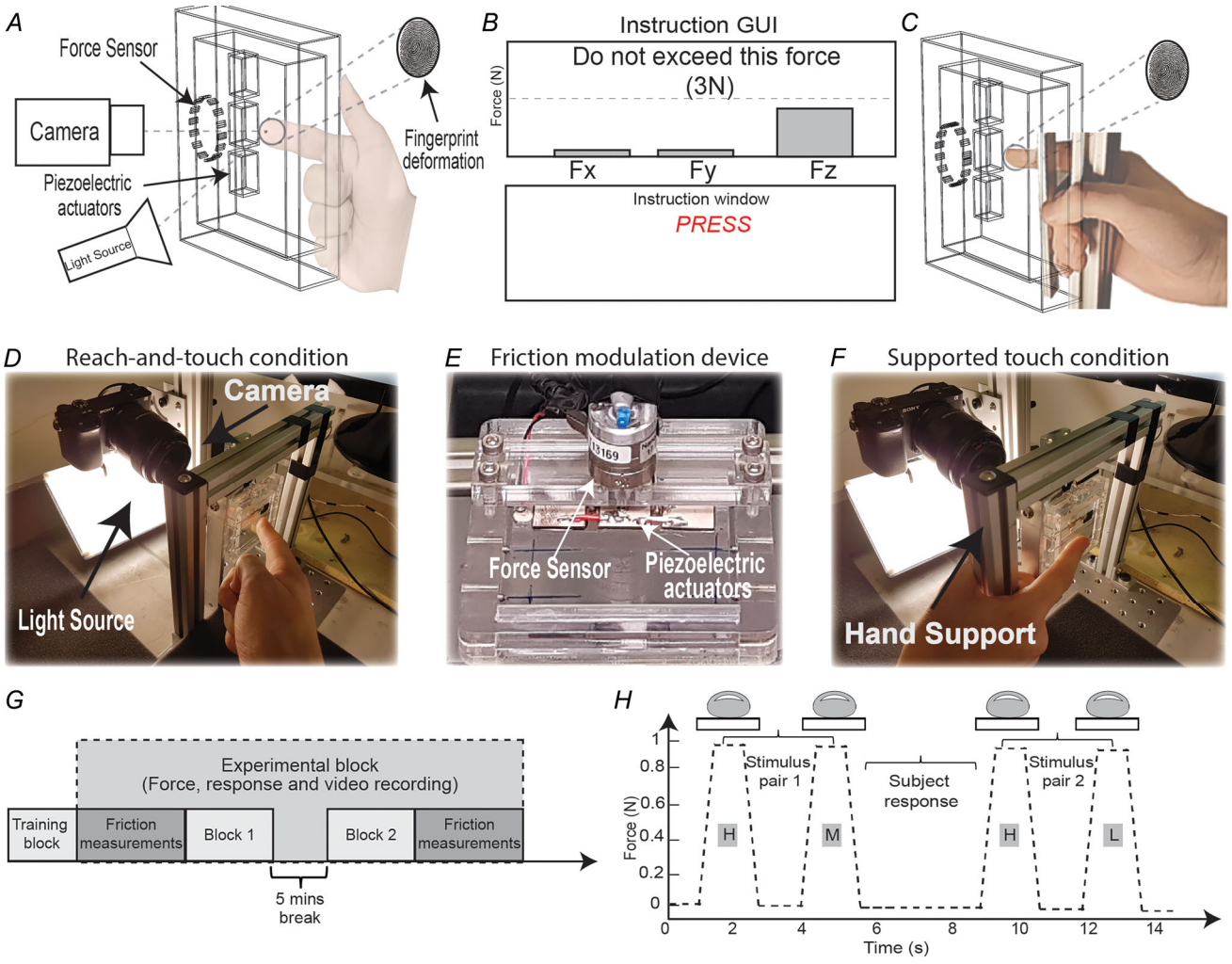

Figure 1. Experimental setup and protocol
A, reach-and-touch condition: illustration of the finger contacting the friction reduction device attached with the piezoelectric actuators modulating the friction of the borosilicate glass mounted on a six-axis force-torque sensor. The light source is positioned under a steep angle to the camera axis to obtain fingerprint images with contrasting ridges and valleys: the light is reflected where there is no skin in contact with the glass of the friction plate, but the light is transmitted (and absorbed by the skin) where skin is in contact with the glass. *B*, a GUI to help pace the timing of when subjects touch, hold and retract skin from the glass. Display of force levels was shown in real-time bar charts to help subjects maintain the desired force level. *C*, supported touch condition: Hand holding a vertical t-slot frame with the thumb, palm and three flexed fingers while touching the friction reduction device using the index finger. *D*, a photo of experimental setup in reach and touch condition. *E*, friction modulation device with three piezoelectric actuators mounted with an ATI-Nano17 Force-torque sensor. *F*, a photo of the experimental setup in the supported touch condition. *G*, schematic of the experimental sequence. *H*, schematic illustration of the time course of presentation and evaluation of the stimulus pairs by subjects touching the friction modulation device (H *vs*. M and H *vs*. L denote pairs of stimuli where H is high friction; L is low friction; M is medium friction). The friction reduction device is switched off for the H condition. [Colour figure can be viewed at wileyonlinelibrary.com]

Data acquisition

Signals from the force/torque sensor, the amplitude of the friction modulation device, and the subject responses were sampled at 1 kHz via another data acquisition unit (PowerLab 16/35; ADInstruments, Bella Vista, NSW, Australia). The fingertip skin deformation profile within the contact area was analysed using video recorded from a Sony α6300 camera (Sony Corporation, Tokyo, Japan) mounted on a frame.

Video capture

Videos of the area of contact between the finger pad and the friction plate were acquired at either 60 frames per second (FPS) (subjects 1 to 5) or 120 FPS (subjects 6 to 12). The camera had a resolution of 1920 $\times$ 1080 pixels and was mounted in a way that resulted in one pixel per 40 $\times$ 40 μm^2 of the scene. High contrast between fingerprint ridges and valleys was obtained by utilising an optical setup that utilised the total internal reflection principle (Fig. 1*A*) (Tada & Kanade, 2004).

Experimental procedure

The subjects were seated comfortably in a height-adjustable chair. The subjects' task was to touch without sliding the vertically-oriented surface of the ultrasonic friction reduction device using the index finger of their right (dominant) hand (Fig. 1*A*). A two-alternative forced-choice protocol (2AFC) was used for the psychophysics study, where two stimuli in a pair, each with a different level of friction, were generated. The timing of when to touch the surface and retract was communicated to subjects by commands on a computer monitor controlled by a graphical user interface (GUI) developed in MATLAB. The force target was shown on the computer monitor using force magnitude progress bars as shown in Fig. 1*B*. The trial started with a command of 'Press' with a beep sound. The subject was then expected to touch the friction reduction device with a target force of ~1 N (Fig. 1*E*). The target force was conveyed to the subjects through the force progress bars on the GUI. A beep sound was generated if the contact force exceeded the 3 N, which happened very rarely. One second after the contact with the surface of the glass was detected, a command to 'Lift' the finger was given in conjunction with the sound cue (beep) for retraction of the finger. After retracting the finger, the next stimulus with a different friction level was presented after a 1 s interval. After the presentation of both stimuli in the pair, subjects verbally indicated which of the two stimuli they felt was more slippery. The responses were recorded by the experimenter.

A training block, comprising 10 pairs of stimuli, was conducted before the start of the experiment to familiarise the subjects with the task. Two different conditions were tested with the same protocol: (1) Reach-and-touch condition (Fig. 1*D*) and (2) Supported-touch condition (Fig. 1*F*). In the reach-and-touch condition, subjects were asked to actively touch the ultrasonic friction reduction device using the right index finger without any exploratory sliding movements. We assigned the term 'reach-and-touch' for this scenario to reflect our aim of investigating the perception of friction within the context of object manipulation. In the process of manipulating objects, our approach involves reaching for the object, establishing a grip, and then lifting it. The complete 2AFC protocol was tested where subjects were instructed to reach and touch the surface of the friction reduction device (Fig. 1*A*). In the supported-touch condition, a hand support was introduced, abolishing the reaching movement, and thus minimising any tangential movements relative to the surface, typically present during a reach and touch movements, as a result of small trajectory deviations from a straight path towards the surface and physiological tremor originating from arm muscles. Subjects were instructed to hold a vertical aluminum t-slot frame with their thumb, palm, and three flexed fingers. In this configuration, they touched the ultrasonic friction reduction device with their index finger by rotation in the metacarpophalangeal joint (Fig. 1*C*). The same 2AFC protocol was used to test the ability of subjects to perceive frictional differences.

Each condition was tested with a total of 60 stimulus pairs. The 60 stimulus pairs for each condition were divided into two experimental blocks, each block comprising 30 stimulus pairs with a 5 min break between each block. Each pair of stimuli (H–M, high *vs*. medium; M–L, medium *vs*. low; H–L, high *vs*. low) was presented 20 times; in 10 trials, the higher friction was presented first followed by the lower friction, and, in the other 10 trials, the lower friction was presented first followed by the higher friction, all presented in a pseudorandom order. Subjects were asked to wear headphones playing white noise to mask auditory cues from the equipment; however, the instructional beeps had sufficient volume to be heard above this white noise. The schematic of the whole experimental protocol is shown in Fig. 1*D*.

Friction measurements and detection of frictional differences by sliding movement

The friction between the fingertip and the contact surface depends upon the accumulation of sweat and several other factors including skin properties (hydration, elasticity, smoothness, etc.). Ten measurements at each friction level (H, M and L) were obtained before and after each experimental block. The stimulus presentation procedure and subject's task were similar to the rest of the trials,

except that, at the end of each trial, instead of lifting their finger off, the subjects were instructed to slide the finger inwards (proximal) to generate a slip. We determined the static coefficient of friction (μ_s) by measuring the tangential-to-normal force ratio at the time when the whole fingertip contact area slipped. The time of slip was determined by visual inspection of force traces and video recording of the fingerprint at the moment when the load force began decreasing.

Image processing

Fingerprint images (Fig. 2*A*) extracted from the video recording were used to detect local movement of the skin over the glass plate of the friction modulation device. Video frames were corrected for perspective by tracking the position of four screws fixed with respect to the glass plate, and a rectangular region of interest encompassing the contact area during the whole contact duration was cropped out. For each touch, a reference video frame was defined as the frame in which the normal force applied was maximal during the contact with the surface. From that reference time, each video recording was split in two sections, before and after the reference frame. Video frames from the reference to the release of the contact, when the finger was retracted, were processed forward in time and frames from first contact (0.1 N normal force) to the reference frame were processed backward; this initiates the tracking algorithm at a time when the grip force was largest and the most fingerprint image features are expected to be present and well identifiable for tracking until they disappear as the region of contact between the skin and the glass shrinks. To enhance contrast in the contact area, the greyscale of each frame was adjusted to cover the range of values present in the contact area of the reference frame. The region of contact between the finger pad and the glass plate was then segmented using a combination of Otsu's thresholding method followed by mathematical morphological operations. The region in which to search for the contact area in a frame was limited to a dilated version of the previous contact area. Within the contact area, features as defined by the minimum eigenvalue algorithm (Shi & Tomasi, 1994) were tracked using the Kanade–Lucas–Tomasi algorithm (Lucas & Kanade, 1981; Tomasi & Kanade, 1991). If the tracking of a feature was interrupted, and resulting trajectories lasted fewer than five frames, those trajectories were discarded from further analysis.

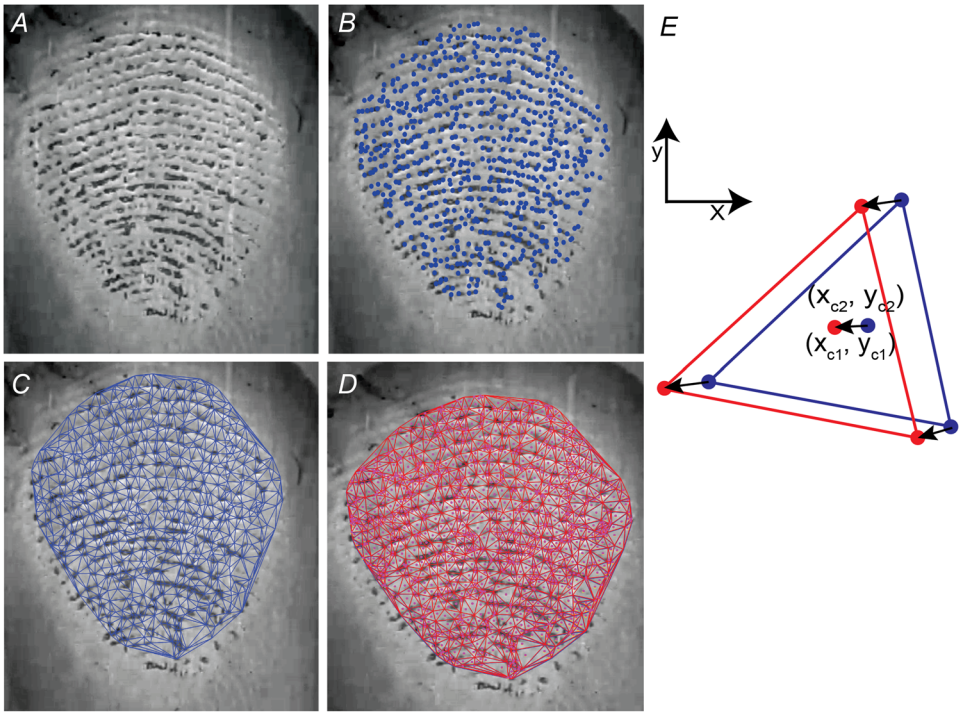

Figure 2. Determining displacement of the skin by fingerprint image analyses
A, an image of the fingerprint within the contact area. *B*, identified feature points used for tracking are shown in blue superimposed on the fingerprint image. *C*, Delaunay triangles are constructed at the current frame joining the tracked feature points (blue triangles). *D*, Delaunay triangles are constructed for the same features which were detected in the next video frame (red triangles). *E*, an enlarged view of the overlapped triangles of the current and next video frame and their incentres. For each triangle, the displacement was calculated based on incentre displacement between two consecutive frames. [Colour figure can be viewed at wileyonlinelibrary.com]

The local displacement of the skin within the contact area was obtained in a three-stage process. (1) In the first step, the positions of valid fingerprint features extracted in sequences of fingertip contact images were segregated (Fig. 2*B*). (2) Using the valid tracked features of the fingerprint, Delaunay triangles were constructed for the consecutive frames (Fig. 2*C* and *D*). The incentre for each triangle was identified and saved for each frame. Using the triangle incentres, displacement vectors were computed for each triangle within each frame (Fig. 2*E*). The area for each triangle was then measured. (3) In the third stage, the slipped triangles were identified by using a displacement threshold of one pixel (Barrea et al., 2018). Any vector with displacement greater than one pixel was considered as a slip and the triangle was regarded as a slipped triangle. The displacement vectors of the incentres of the triangles were calculated for each frame.

Skin displacement magnitude

The skin displacement magnitude was calculated by assigning each pixel within a Delaunay triangle with a displacement vector equal to the movement of the triangle's incentre. The triangle displacement in the current frame was calculated with respect to its position in the previous frame. We introduced several measures to quantify the skin displacement patterns estimated on a pixel-by-pixel basis in images of the contact area: (1) total displacement; (2) net displacement; (3) displacement jitter; and (4) divergence.

Total and net displacement. First, we calculated the pixel displacement vectors $\vec{P} = (P_x,\ P_y)$ and their norms $\|\vec{P}\|$ for each pixel i in each frame j. Thus, each pixel displacement vector represents the vector difference of the co-ordinates of a point on the skin between two consecutive frames. All the pixel displacement vectors are summed for each frame and represented as f_{net_j} and their norms are summed and represented as f_{total_j} mathematically:

$$f_{net_j} = \left\| \sum_{i=1}^{m} \vec{P_i} \right\| \tag{1}$$

$$f_{total_j} = \sum_{i=1}^{m} \left\| \vec{P_i} \right\| \tag{2}$$

where m is the total number of skin contact area pixels in the frame.

The total displacement f_{total_j} measure represents the cumulative distance that all the pixels covering the whole field of points within the skin contact area have slid over the surface regardless of direction in which each point moved. This characterises the extent to which tactile receptors have been stimulated by skin slippage.

The net displacement f_{net_j} represents the vector sum of all pixel size point movement denoting the length of the resultant vector indicating the magnitude of the contact area centre displacement.

Displacement jitter (*DJ*) in the present study characterises the frame-by-frame deviation of the contact area centre displacement path from a straight line of displacement, between first and last frames of the entire movement. The displacement jitter was quantified by taking a norm of the net displacement vector estimated for each frame then summed across all frames and subtracting the norm of the net displacement vector between the start and end frames, estimated as the vector sum of all pixel-size point displacements:

$$DJ = \sum_{j=1}^{k} \left\| \sum_{i=1}^{m} \vec{P}_{ij} \right\| - \left\| \sum_{j=1}^{k} \left(\sum_{i=1}^{m} \vec{P}_{ij} \right) \right\| \tag{3}$$

where k represents the total number of frames.

Divergence (*D*). The skin displacement in a divergence pattern in the present study was calculated by taking the difference between the total cumulative displacement and the net cumulative displacement between each pair of frames and then summed across all the frames analysed:

$$D = \sum_{j=1}^{k} \left(f_{total_j} - f_{net_j} \right) \tag{4}$$

The D measure in our study denotes skin displacement which doesn't contribute to the net skin displacement within the contact area. It is primarily the radial inside-out contact area expansion (Willemet et al., 2021) but may also include some less important symmetrical displacement patterns.

Statistical analysis

First, we estimated a quotient $Q_{\mu s}$ of static coefficients of friction μ_s for each pair of frictional stimuli. A one-sample t test was performed to confirm that the $Q_{\mu s}$ was significantly different from 1 and thus μ_s values for the two stimuli in a pair are different (where $Q_{\mu s} = 1$, this would indicate that the measured μ_s values for two stimuli in a pair are equal). Analysis of variance (ANOVAs) and *post hoc* paired sample tests (with Bonferroni corrected values for multiple comparisons) were performed if a comparison of more than two groups was required. Fractional degrees of freedom are reported accordingly to the Greenhouse–Geisser correction when Mauchly's test of sphericity showed that the assumption of sphericity had been violated. When a D'Agostino–Pearson normality

test ($P < 0.05$) indicated that the data was not normally distributed, instead of ANOVA, the Friedman test was used. A Wilcoxon matched pairs signed-rank test was used as a non-parametric alternative to the *t* test when differences between two groups had to be evaluated.

Results

Frictional properties of the contact between the fingertip skin and surface are individual and depend upon several variable factors including skin mechanical properties and the amount of sweat. Thus, we first had to assess the actual frictional difference and efficacy of ultrasonic friction modulation between the pairs of stimuli. Then, we reported the ability of subjects to differentiate between two frictional levels by reporting which surface felt more slippery when reaching and touching the surface (reach-and-touch condition). By means of biomechanical analyses of the fingertip skin strain patterns during the touch, we observed that the source of sensory input determining the ability of subjects to differentiate slipperiness of two surfaces relates to the presence of partial slips. In the follow-up experiment, in which we restricted movement to finger only (supported touch), we determined that natural reaching movement kinematics is at the heart of the friction sensing mechanism at the initial touch.

Reach-and-touch condition

Frictional effect achieved by friction reduction device. The frictional measurements were obtained by subjects contacting the friction reduction device surface and sliding their fingers in the proximal direction. The mean measured coefficient of static friction (μ_s) during the reach-and-touch experimental block was 0.65 ± 0.27, 0.48 ± 0.22 and 0.29 ± 0.14 (mean ± SD) for high (H), medium (M) and low (L) friction conditions, respectively. The ratio of the larger measured μ_s to the smallest measured μ_s for the two stimuli in a pair (i.e. a quotient $Q_{\mu s}$) varied amongst subjects, ranging between 1.12 and 1.61 for H *vs.* M, between 1.42 and 2.20 for M *vs.* L, and 1.70 and 3.51 for H *vs.* L friction levels (minimum to maximum, respectively) (Fig. 3*A*). A one-sample *t* test for each of the frictional combinations indicated that $Q_{\mu s}$ was significantly different from 1 (H–M, $P = 0.0001$; M–L, $P < 0.0001$; H–L, $P < 0.0001$, $n = 11$) indicating that the μ_s values of the stimuli presented in every pair were significantly different. It is also apparent that the largest measured frictional differences were in H–L followed by M–L and the smallest differences were measured in H–M pairs of stimuli. It should be noted that exact frictional differences cannot be controlled and will inevitably vary between subjects and from trial to trial.

Subjects' ability to discriminate friction. The friction discrimination ability of the individual subjects during the reach-and-touch condition for the three pairs of stimuli are shown in Fig. 3*B*. The overall accuracy across subjects was 87 ± 8% (mean ± SD; $n = 11$). For the pairs of stimuli with the largest frictional difference (H–L), all 11 subjects performed above 75% performance level (95 ± 6%). The discrimination performance between the two stimuli with a smaller frictional difference, H–M and M–L, remained high and was 79 ± 11% and 87 ± 13%, respectively (mean ± SD). There was a significant difference between the performance of the subjects among

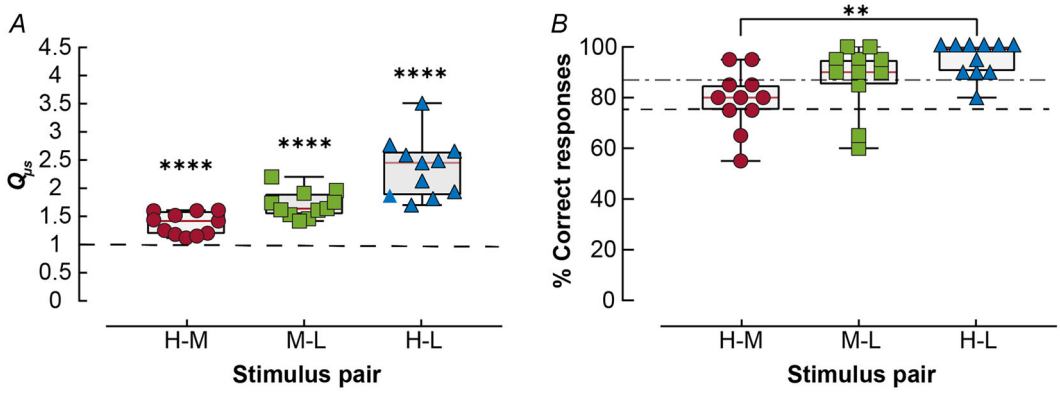

Figure 3. Friction discrimination in the reach-and-touch condition
A, boxplots displaying the median and quartile range of $Q_{\mu s}$ (quotient of the larger and smaller mean μs for the two stimuli in a pair) measured for individual subjects ($n = 11$). Dashed horizontal black line across the graph is $Q_{\mu s} = 1$ (i.e. if two stimuli in a pair would have equal μ_s). ****Significant difference between mean $Q_{\mu s}$ and 1 at $P < 0.001$; one-sample *t* test. *B*, boxplots displaying the median and quartile range of percentages of correct responses across friction pairs for reach-and-touch condition. Individual subject data are shown by symbols ($n = 11$). Dashed horizontal black line represents selected 75% performance threshold level. Dash-dotted line represents the mean of all subjects across stimulus pairs. **$P <= 0.001$ (Bonferroni corrected). [Colour figure can be viewed at wileyonlinelibrary.com]

the three pairs of stimuli (one-way repeated-measures ANOVA, $F_{1.594,15.94} = 11.58$, $P = 0.0013$). *Post hoc* analyses indicated that the performance differed only between stimulus pairs of highest and smallest frictional difference (H–M *vs.* H–L, $P = 0.0010$) and was similar between pairs of intermediate differences (H–M *vs.* M–L, $P = 0.1764$; M–L *vs.* H–L, $P = 0.0709$; Bonferroni-corrected multiple comparisons). Only two subjects, S3 and S4, had a performance below the 75% threshold (55% and 65%, respectively) for the H–M stimulus pairs, and subjects S3 and S2 in the M–L pairs of stimuli, (65% and 60%, respectively). The possible reason could be that the frictional difference between the low performing pairs for S3 was relatively small. The mean $Q_{\mu s}$ was 1.25 for the H–M pair and 1.46 for the M–L pair, being among the lowest measurements for all subjects. The performance of these subjects in H–L trials with larger frictional differences was well above the 75% performance level.

Skin deformation leading to partial and gross slips. To identify the role of friction-dependent skin deformation and localised slips that signal frictional properties of the surface, we used the fingerprint image analyses and tracked displacement of identified fingerprint image features. Subjects reached and touched the stimulus surface having being instructed that sliding lateral finger movements are not allowed and that they must touch the surface in a manner similar to that when gripping an object for manipulation. Because friction can only be measured when there is a relative motion between the contact surfaces, partial or gross slip, we first computed the portion of the fingerprint area that slipped over the time course of making the contact. The point in time when the largest amount of slip occurred potentially comprises the best source of information for shaping the friction perception. The relative size of the fingertip skin contact area that slipped when touching the surface over the duration of the trial is shown in Fig. 4*A*.

Regardless of frictional condition, 100 ms after touching, the surface the area of fingertip skin contacting the surface was 70% of its maximum size reached later during the trial. However, ∼40% of the current skin contact area was slipping in the low friction condition, but only 10% was slipping in the high friction condition. This indicates that the fraction of partial slippage relative to the total skin area contacting the surface at this time point reflected the frictional condition. The fingerprint image analysis at the very first frame, after 0.1 N of contact force was detected, was not performed because fingerprint features at such low contact force were not reliably discernible yet. Therefore, it cannot be excluded that gross slips predominate during this period. The slip detection analyses are performed for feature displacements detected between video frames 2 and 3 (at 60 fps this is 49.98 ms after contact is detected) (Fig. 4). The largest fraction of skin area slipping was observed during the first 100 or 200 ms of the contact, which is the time interval most critical for obtaining frictional information to control fingertip forces during object manipulation. The amount of initial slippage was clearly related to the frictional condition: a larger part of the contact area slipped when the friction was low (L) and, conversely, a lesser amount of skin slipped when the friction was high (H). With the high friction surface, typically, all parts of the skin maintained stable contact after the first 100 ms. Figure 4*B* summarises the percentage area slipped and variability between subjects at 100 ms after the contact was made. It can be clearly seen that the slipped contact area was notably larger when the friction was low, and it became smaller as the friction increased. After the first 100 ms, on average, 40.49 ± 16.08%, 20.43 ± 13.54% and 5.02 ± 4.65% of contact area was slipping with H, M and L frictional surfaces, respectively. A one-way repeated-measures ANOVA indicated that the difference was significant ($F_{1.705,17.05}) = 32.57$, $P = 0.0001$). *Post hoc* analyses revealed that the area slipped was significantly different between two surfaces presented in pairs H–M, M–L and H–L (H < M, $P = 0.0031$; M < L, $P = 0.0053$; H < L, $P = 0.0001$, respectively; Bonferroni-corrected for multiple comparisons). In the majority of instances, these were partial slips.

The probability of having a gross slip (defined as at least 90% of the contact area slipping) is shown in Fig. 4*C*. It is apparent that only 16% of the trials in the low friction condition have gross slips at the start of the trial, which shows that subjects have followed the instructions and this is not an intentional exploratory lateral sliding movement. After this initial period, the contact stability increased and gross slips were rare. The normal force increase rate during the first 100 ms of contact was 6.21 ± 3.44, 6.24 ± 3.38 and 6.92 ± 4.06 N s^{-1} (mean ± SD) during H, M and L frictional levels, respectively; thus being similar and not affected by the frictional level ($F_{1.580,15.80} = 1.486$, $P = 0.2532$; one-way ANOVA). At the time point of the third video frame, when the image processing began, the normal force already reached ∼0.4 N on average (Fig. 4*D*).

Supported touch

Based on the observations above, we established that, in the absence of intentional exploratory movements, some skin displacement and partial slips were unavoidably present. This indicates that tangential components of the movement kinematics, although small, could potentially be sufficient to enable subjects to evaluate and discriminate frictional properties of the surfaces. This is supported by submillimetre range displacement between the object's surface relative to the rigid nail-phalangeal

bone complex probably having such an enabling effect. To test whether movement kinematics indeed play a decisive role in friction sensing and perception, we designed an experiment in which we restricted the trajectory of finger movement by introducing a hand support, thus reducing natural, but experimentally unwanted, lateral movement components. With the introduction of the hand support, no reaching movement was present. It also served to minimise the effects of physiological tremor originating from the large arm muscles. Thus, any tangential finger movements relative to the surface were minimised, constraining it to a straighter path. This condition is termed 'supported touch condition', where the stimulus surface is touched by moving a finger while the palm of the hand and last three fingers enclose the hand support rod (Fig. 1*C*). We start by reporting the subjects' performance changes after the introduction of the hand support, then analyse the extent of changes in skin displacement and, finally, aiming to establish causality between skin displacement and subjects' performance, we analyse whether stochastic trial-to-trial variation in displacement can be linked to subjects' performance.

Frictional effect on skin from friction reduction device. The static coefficient of friction measured for each of the three rendered friction levels (H, M, and L) was different among subjects. The measured coefficient of friction (μ_s) was 0.65 ± 0.28, 0.53 ± 0.25 and 0.35 ± 0.18 (mean ± SD) for supported touch. The ratio of the larger measured μ_s to the smallest measured μ_s (i.e. $Q_{\mu s}$) for the two stimuli in a pair varied amongst subjects,

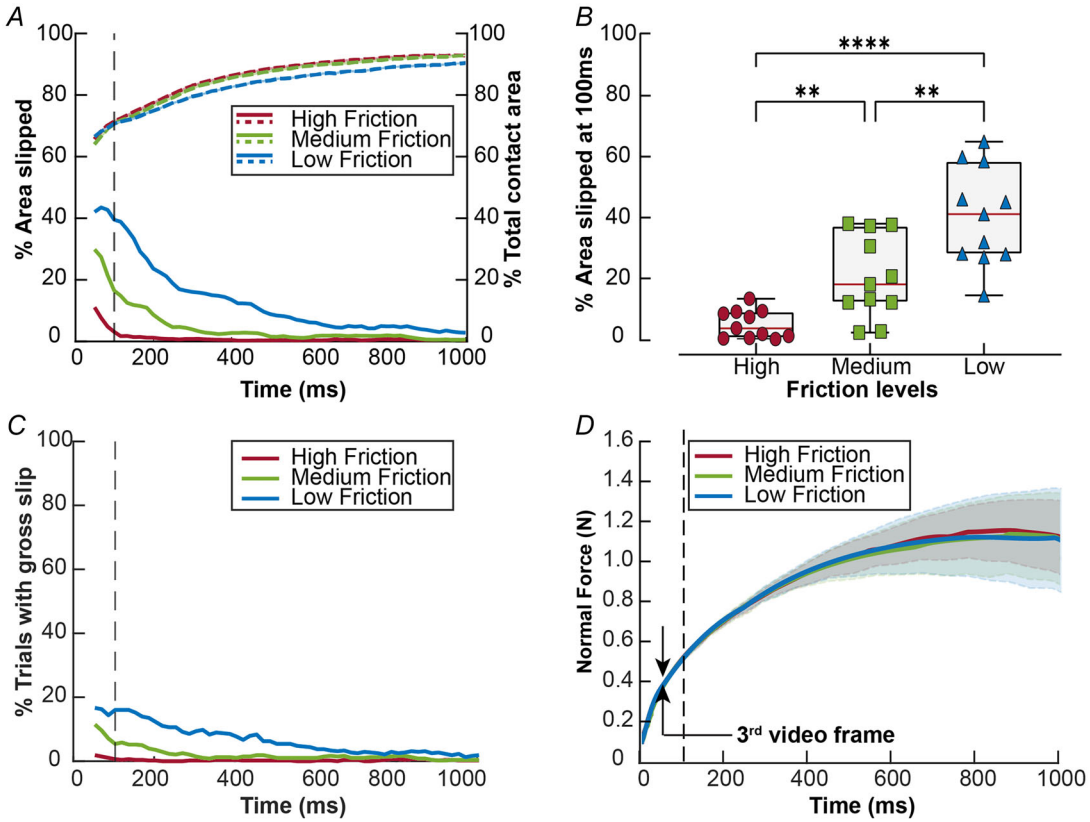

Figure 4. Temporal evolution of fingerprint contact area slipped and normal force development in the reach-and-touch condition
A, mean of the percentage area slipped during the reach-and-touch movement from the initial touch over the duration of the trial (colour-coded lines at the bottom of the graph). The right-side *y*-axis and dashed lines at the top represent the total contact area growing throughout the touch trial. The fingertip skin displacement measures are first estimated at third video frame relative to the second frame, which is 49.98 ms after the detection of the initial contact at 0.1 N. The first video frame was ignored as fingerprint features were not reliably discernible. *B*, boxplots displaying the median and quartile range of the percentage area slipping for individual subjects after the first 100 ms of touch, corresponding to the dashed vertical line in (*A*) (n = 11). ****$P \leq 0.00001$ (Bonferroni corrected). *C*, proportion of trials in which gross slip (defined as at least 90% of the contact area slipping) was detected at each time point during the trial. *D*, normal force development over the duration of contact. The vertical line indicates the 100 ms time point after the initial contact. Solid lines indicate the mean across all subjects (n = 11) and shaded areas indicate the SD. [Colour figure can be viewed at wileyonlinelibrary.com]

ranging between 1.05 and 1.53 for H–M, between 1.25 and 2.06 for M–L, and 1.32 and 3.03 for H–L (minimum to maximum, respectively) during the supported touch condition (Fig. 5*A*). A one-sample *t*-test for each of the frictional combinations indicated that there was a significant difference between the mean $Q_{\mu s}$ measured in the supported touch condition (H–M, $P = 0.0003$; M–L, $P < 0.0001$; H–L, $P < 0.0001$, $n = 11$), meaning that the μ_s values of the stimuli presented in pairs were significantly different.

Subjects' ability to discriminate friction. As a result of the introduction of the hand support, the friction discrimination ability of the individual subjects significantly deteriorated (Fig. 5*B*) compared to the reach-and-touch condition (Fig. 3*B*). For the pairs of stimuli, even with the largest frictional difference (H–L), only five out of 11 subjects performed above the 75% threshold. On average, the performance for the H–L friction pair was just above 75% (77.73 ± 18.89%) and considerably lower than in the reach-and-touch condition (95 ± 6%; mean ± SD) for the pairs of stimuli with the largest frictional difference (H–L). The discrimination performance between two stimuli with smaller frictional differences H–M and M–L on average was below the 75% threshold, being 67.73 ± 16.64% and 64.55 ± 13.50%, respectively. On average, across three levels of frictional differences, the subjects' performance was 66.14% ± 12.01%. One-way repeated-measures ANOVA ($F_{1.535,15.35} = 4.233$, $P = 0.0429$) and *post hoc* analyses indicated that the only difference in performance was between the pairs of smallest and largest frictional differences ($P = 0.0341$ for M–L *vs.* H–L; Bonferroni-corrected multiple comparisons). Two-way-repeated-measures ANOVA ($F_{1,10} = 9.648$, $P = 0.011$) (Fig. 5*C*) indicated that the performance differed significantly between the two touch conditions. There was no interaction between the touch conditions and the rendered friction levels ($F_{2,20} = 0.538$, $P = 0.591$). The poor performance of subjects under constrained movement kinematics was explained by a significantly reduced amount of typically submillimeter range lateral movements and by the extent of partial slips.

Skin deformation leading to partial and gross slips. The constraints imposed on the movement kinematics substantially affected skin displacement magnitude after contact with the surface, which might explain the poor performance of subjects in discriminating the friction difference of the stimulus pairs. The mean percentage of area slipped for all the subjects over the 1 s duration of the contact is shown in Fig. 5*D*. Overall, the contact with the stimulus surface was very stable, with reduced movement of the fingers over the duration of the whole trial, compared to the unrestrained reach-and-touch condition. It can be observed that, after the initial touch with a surface, there appears to be no further slip or even partial slip present in the supported touch condition compared to the reach-and-touch condition where small amounts of partial slip were present throughout the trial. At 100 ms after initial contact was made (Fig. 5*E*), on average, 10.70% ± 6.35%, 3.08% ± 2.87% and 1.55% ± 2.24% of the contact area was slipping during the H, M and L frictional levels, respectively. One-way repeated-measures ANOVA indicated that the mean percent area slipped was significantly different between H, M and L frictional levels at 100ms after the initial contact was detected ($F_{1.066,10.66} = 21.89$, $P = 0.0006$). *Post hoc* analyses revealed that the area slipped was significantly different between any two rendered friction levels (H < M, $P = 0.0316$; M < L, $P = 0.0024$; H < L, $P = 0.0025$, respectively; Bonferroni-corrected for multiple comparisons). Regardless of frictional effects, the size of the area that slipped was relatively small and appeared to be insufficient for the subjects to base the decision on which surface was more slippery. In comparison with the reach-and-touch condition, the area slipped in supported touch was only 26%, 15% and 30% compared to that in the reach-and-touch condition. Gross slip was observed only with the low friction surface in 5% of trials (Fig. 5*F*). Gross slips were almost fully absent with the medium and high friction rendered surfaces. The normal force increase rate during the first 100 ms of contact was 4.26 ± 3.18, 4.09 ± 3.11 and 4.70 ± 3.30 N s^{-1} (mean ± SD) during H, M and L frictional level, respectively, thus being very similar and not affected by the frictional level ($F_{1.724,17.24} = 1.795$, $P = 0.1980$; one-way ANOVA).

Effect of hand support on skin displacement magnitude and slip patterns. To further demonstrate how fingertip skin displacement and slip patterns reflect frictional differences, fingerprint image feature tracking was performed. Figure 6 shows example patterns of local skin displacement magnitude when touching surfaces with high and low friction (Fig. 6*A vs. B*; *C vs. D*) and compares the effects between reach-and-touch *vs.* supported touch conditions (Fig. 6*A* and *B vs. C* and *D*). When touching the high friction surface, the local skin displacement is negligible and does not exceed a magnitude of ∼0.1 mm. However, with the low friction surface, at some time during the trial, most of the skin area in contact with surface has slipped, although the extent of slip displacement depended on the type of touch. During the reach-and-touch condition, the displacement is substantial, reaching ∼0.8–1.0 mm in magnitude, whereas, in supported touch, the slip is considerably smaller (∼0.1 mm).

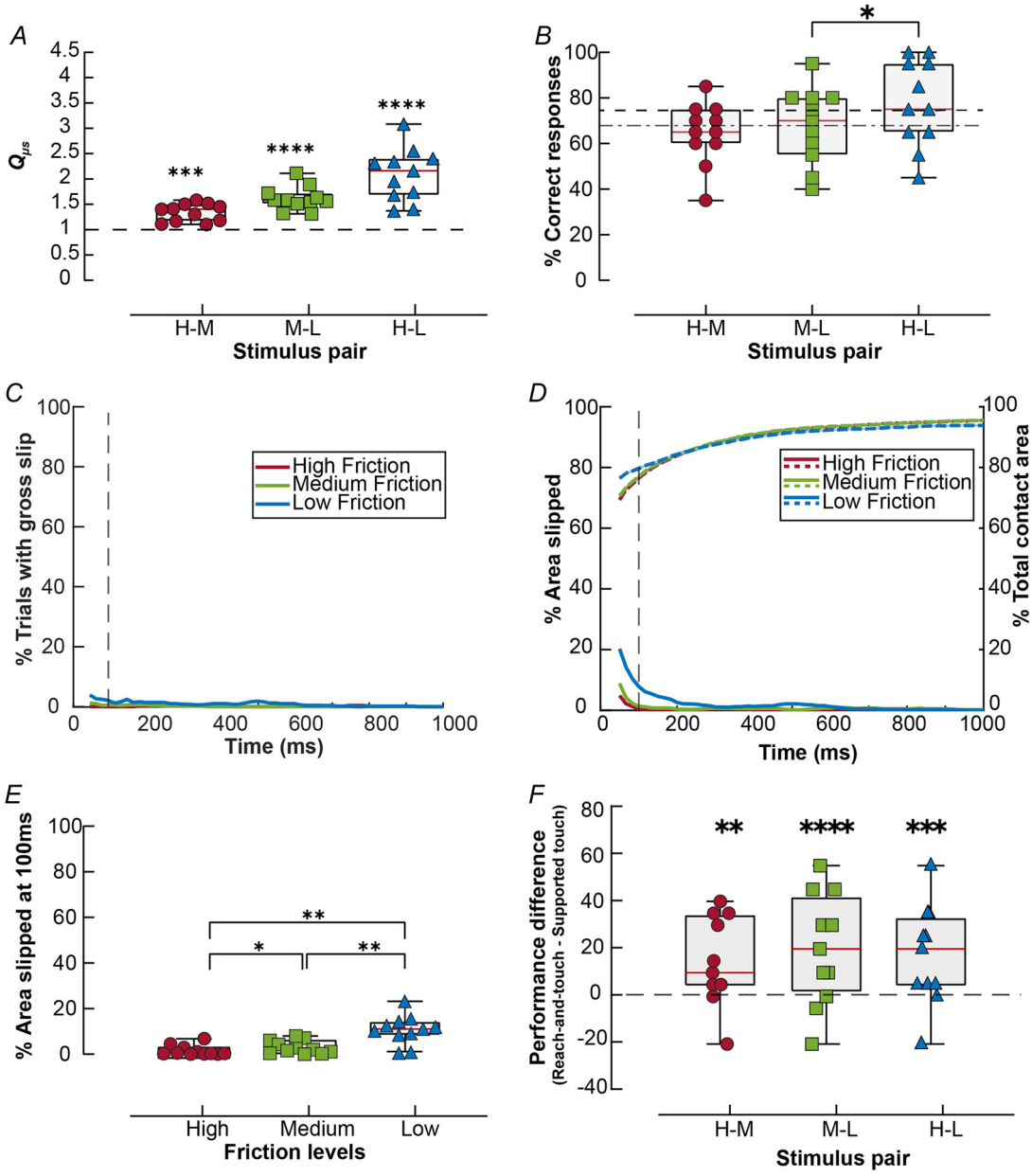

Figure 5. Subjects' performance and fingerprint contact area slipped in the supported touch condition
A, boxplots displaying the median and quartile range of the quotient of the coefficient of friction measured for individual subjects (n = 11). Symbols show data from individual subjects (n = 11). Dashed horizontal black line across the graph is $Q_{\mu s}$ = 1 (i.e. if two stimuli in a pair would have equal μ_s). ****Significant difference between the mean $Q_{\mu s}$ and 1 at $P < 0.001$; one-sample t test. *B*, boxplots displaying the median and quartile range of percentages of correct responses across friction pairs for the supported touch condition. Dashed horizontal black line represents 75% performance threshold level. Dash-dotted line represents the mean performance of all subjects across all stimulus pairs. *C*, proportion of trials in which gross slip was detected as a function of time after the initial contact. The vertical dashed line indicates 100 ms after initial contact with the surface. *D*, mean of the percentage area slipped during the reach-and-touch movement from the initial touch over the duration of the trial (colour-coded lines at the bottom of the graph). The vertical line indicates the initial phase of the contact at 100 ms. The right-side y-axis and dashed lines at the top represent the total contact area growth over the duration of the touch trial. *E*, boxplots displaying the median and quartile range of the percentage area slipping for individual subjects after the first 100 ms of touch corresponding to the dashed vertical line in (*A*) (n = 11). *F*, boxplots displaying the median and quartile range of performance difference between the reach-and-touch condition and the supported touch condition across friction pairs. ****$P < 0.0001$ (Bonferroni corrected). [Colour figure can be viewed at wileyonlinelibrary.com]

Skin displacement measured over the duration of whole trial. The total displacement of skin segments over the whole duration of the trial was much less for the supported touch condition compared to the reach-and-touch condition. The relative fraction of the total skin displacement in the supported touch condition was 0.19 (0.11–0.45), 0.08 (0.04–0.32) and 0.09 (0.06–0.18) [median (quartile)] compared to that in the reach-and-touch condition, with H, M and L friction levels, respectively (Fig. 7*A*). As an exception, in two out of eleven subjects, the movement resulted in larger skin displacement in the support condition. A Wilcoxon matched-pairs signed-rank test performed on the measured values of the total displacement of skin segments between the reach-and-touch condition and supported touch condition indicated that there was a significant difference at each of the three friction levels (H, $P = 0.0419$; M, $P = 0.0244$; L, $P = 0.0009$).

In the local skin displacement pattern, we specifically discerned a divergence and small displacement jitter, which might partly arise from physiological tremor. Radial divergence of the skin will occur during the skin–object contact because of the approximately hemispherical shape of the fingertip. The extent of divergence depends on the friction. The fraction of divergence relative to the total displacement during the reach-and-touch condition was 0.15 (0.11–0.30), 0.07 (0.03–0.12) and 0.03 (0.02–0.07) [median (quartile)] during H, M and L friction levels, respectively. In the supported touch condition, the divergence measured relative to the total skin displacement was 0.25 (0.14–0.30), 0.07 (0.03–0.12) and 0.03 (0.02–0.07) [median (quartile)] during H, M and L friction levels, respectively. In both grip configurations, the effect of friction on divergence was statistically significant ($Q = 18.73$, $P < 0.0001$ reach-and-touch condition; $Q = 11.64$, $P = 0.0014$ supported touch condition; Friedman test). The relative difference of the divergence between the two conditions (i.e. the ratio of the divergence measured for the supported touch condition to the divergence measured for the reach-and-touch condition) was 0.31 (0.25–0.60), 0.28 (0.15–0.63) and 0.32 (0.15–0.53) [median (quartile)] during H, M and L friction levels, respectively (Fig. 7*B*), indicating that divergence observed in the supported touch condition was one-third of what it was in the reach-and-touch condition. This indicates that increased lateral movement present in the reach-and-touch condition facilitated the release of radial stress within the contact area.

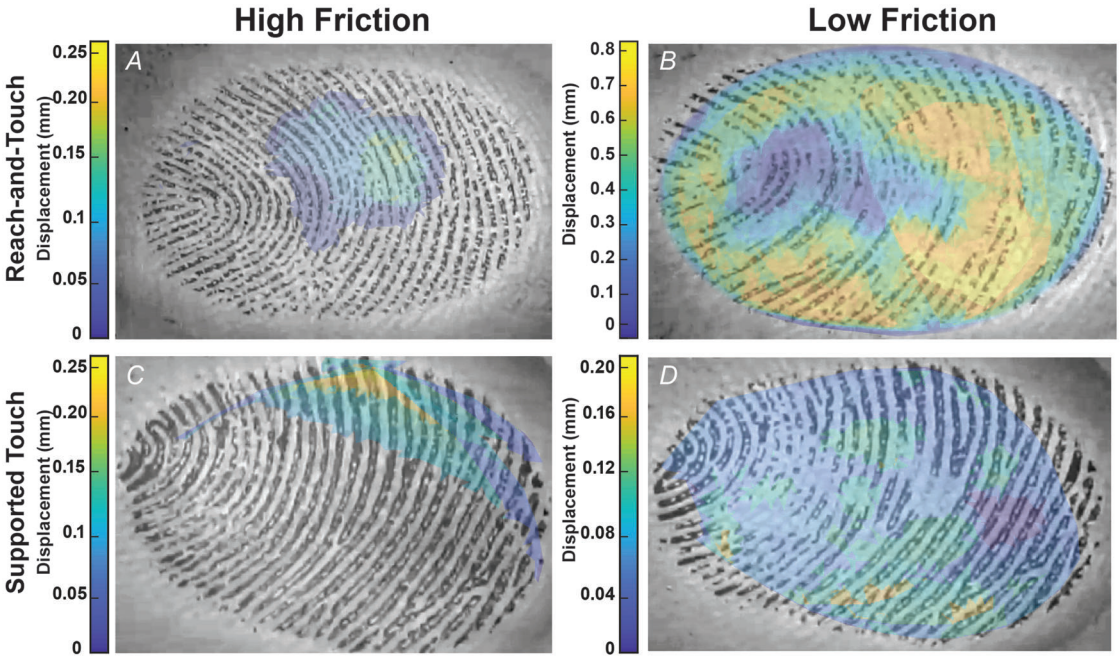

Figure 6. Local displacement magnitude pattern of the fingertip skin touches high and low friction surfaces during reach-and-touch and supported touch condition trials
The heat map represents the local displacement magnitude measured between the first video frame, when each fingerprint feature was identified, and the last video frame overlaid on top of the fingerprint image. More displacement was observed in the low friction condition compared to the high friction condition across both experimental conditions. However, greater overall displacement was observed in the reach-and-touch condition than in the supported touch condition. *A* and *B*, high friction and low friction in the reach-and-touch condition. *C* and *D*, high friction and low friction in supported-touch condition. [Colour figure can be viewed at wileyonlinelibrary.com]

The fractional contribution of displacement jitter of the fingers to the total skin displacement was 0.08 (0.06–0.14), 0.11 (0.08–0.14) and 0.17 (0.11–0.27) in the reach-and-touch condition and 0.09 (0.03–0.13), 0.08 (0.04–0.17) and 0.11 (0.09–0.16) in the supported touch condition [median (quartile)] with H, M and L friction levels). This indicates that, overall, the contribution of the displacement jitter to the total skin displacement was negligible in most cases.

The ability of subjects to discriminate frictional properties is correlated with stochastic variation of skin area slipped. To evaluate whether subjects' performance was influenced by the stochastic variation in the size of the area slipped we analysed and compared area slipped between two surfaces in the pair during trials in which subjects correctly and incorrectly identified the more slippery surface. First, we estimated the difference in percent slipped area by subtracting the area slipped (expressed as percentage of the total area) when touching the less slippery surface from the area slipped for the more slippery surface in the pair. Data from both reach-and-touch and supported touch conditions were used in these analyses. The difference in percent slipped area for each pair of stimuli during correct and incorrect trials is shown in Fig. 8 (left). When the responses were correct, the difference in percent slipped area was consistently higher in the trials where subjects identified frictional differences correctly compared to the trials where subjects were unable to discriminate frictional differences (Fig. 8, right). This demonstrates that the ability of subjects to discriminate friction of two surfaces was clearly related to and probably determined by the stochastic variation in the size of partial slip differences.

Discussion

Sensing friction between fingertip skin and a surface may serve two purposes: to explore characteristics of a material or to control grip forces when manipulating an object held in the hand. The same physical feature, friction, is sensed under different sensory conditions. To evaluate the physical characteristics of a material, we slide our fingers over the surface, creating a perceptual experience. Object manipulation, however, does not permit such exploratory movements and frictional information should be obtained just by touching the surface. Grip force adjustments to friction are largely automatic (Birznieks et al., 1998) and thus in principle do not necessitate cognitive involvement. Nevertheless, some associated awareness of grip surface slipperiness is present, which is perceptually similar to that felt during exploratory sliding or rubbing finger movements over surfaces. Knowledge of slipperiness can be critical for the selection of a safe and achievable action plan ensuring that, when performing an intended manipulation, the required grip forces to hold an object or tool safely would not exceed the hand's physical ability to produce them or not exceed the breakage point of fragile objects.

Previous studies have demonstrated that the ability of humans to differentiate the frictional properties of two otherwise identical materials when touching them might be challenging and depend on multiple factors. In the case of well-controlled stimuli (i.e. when a robotic manipulator brought a surface in contact with the finger pad skin), the subjects were unable to differentiate their frictional properties. This was demonstrated when friction was changed using a friction modulation device (Wiertlewski

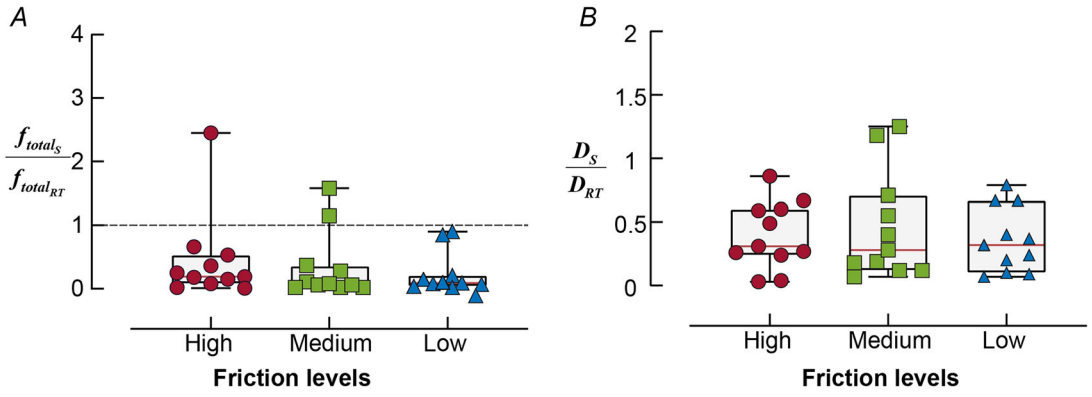

Figure 7. Comparative skin displacement analysis between two touch conditions: total skin displacements and skin divergence
A, boxplots represent the median and quartile range of the fraction of the total skin displacement after the hand support was introduced for each of three friction levels. f_{total_S} represents the total skin displacement measured during the supported touch condition and $f_{total_{RT}}$ represents the total skin displacement measured during the reach-and-touch condition. *B*, boxplots represent the median and quartile range of the fraction of skin divergence after the hand support was introduced for each of three friction levels. D_S represents the divergence measured during the supported touch condition and D_{RT} represents the divergence measured during the reach-and-touch condition. [Colour figure can be viewed at wileyonlinelibrary.com]

et al., 2016) with either smooth surfaces or with surface textures (Khamis et al., 2021). Even changing the approach angle of the robotic manipulator from perpendicular to 20° and 30° from normal (producing 8.9° and 19° force angles and 0.47 ± 0.07 mm lateral movement after the first contact was detected) did not improve performance. In the follow-up study using the same experimental setup in which a robotic manipulator brought a surface to an immobilised finger, it was found that a sub-millimeter range lateral movement as small as 0.5 mm and, in some subjects, just 0.2 mm of the surface relative to the affixed rigid nail-phalangeal bone complex was sufficient to enable the subjects to differentiate surfaces based on their slipperiness (Afzal et al., 2022). Such small tangential movement deviations from a straight path when making contact with a surface are expected to occur during natural movement when humans reach and touch object surfaces. Based on that, in the present study, we tested the hypothesis that natural reaching movement kinematics would have an enabling effect to sense the slipperiness of smooth surfaces when no other sensory cues are available. It has to be recognised that the fact of the presence of such tangential sub-millimeter range movements does not mean that it would necessarily enable subjects to differentiate friction due to the stochastic unpredictable nature of these movements in comparison to the experimental setup where applied displacements were reproducible, controlled by a robot, and thus identical. When subjects themselves touch surfaces, there would be trial-to-trial variability in several contact parameters, including the magnitude of tangential displacement, adding complexity to the sensory signal from which differences in slipperiness have to be derived.

In the present study, active movements enabled subjects to perceive differences in the slipperiness of surfaces that they were previously unable to differentiate in a passive condition (Khamis et al., 2021). We also demonstrated that, in most cases, partial slips were sufficient to make the judgement. Gross slips occurred in the minority of trials and skin displacements were over very small distances, confirming that subjects followed the instructions and did not attempt to use exploratory sliding movements. Partial slips were especially prominent in the early phase when contact with the surface was made, thus being the most informative period for receptors to signal frictional properties of the surface. The fingerprint image analyses for identifying skin deformation and slips became available only after the first two video frames (∼32 ms) of the contact when contact with a sufficient grip force was made and fingerprint features became discernible. Thus, some finger sliding over the surface might have occurred that potentially could provide rich sensory information. Single afferent recordings in humans (micro-neurography studies) and psychophysics experiments employing controlled stimuli may reveal the relative importance of these mechanical events. Additionally, higher activation levels in three prefrontal cortex regions, during the early phase of contact, suggests a crucial role for these regions in processing tactile information related to slipperiness perception (Zhou et al., 2023).

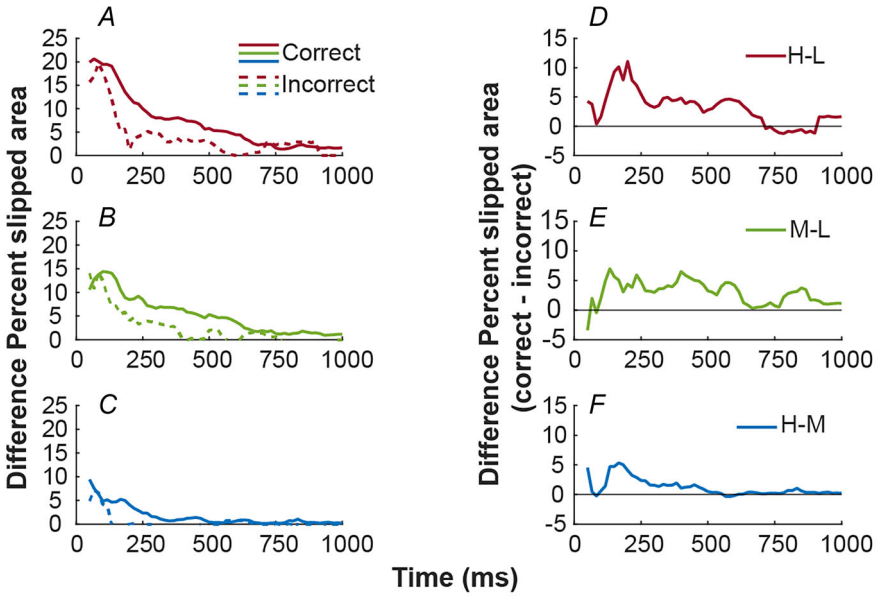

Figure 8. Difference percent slipped area between two surfaces in the friction pair over the course of trial during correct and incorrect trials
Difference in percent slipped area for H–L (*A*), M–L (*B*) and H–M (*C*) frictional pairs. Solid lines represent correct trials and dashed lines incorrect trials. The panels on the right (*D–F*) show the difference in percent slipped area in incorrect trials subtracted from the correct trials. [Colour figure can be viewed at wileyonlinelibrary.com]

The ability of subjects to evaluate slipperiness of surfaces dramatically deteriorated when movement constraints were introduced, and the contact was made by finger movements with limited lateral deviation from a straight path. For most subjects, performance fell to the chance level, demonstrating that natural reaching movement kinematics played a decisive role in enabling the subjects to evaluate surface frictional properties. Constrained finger movement paths significantly reduced skin displacement: the size and extent of the partial slips. Furthermore, the analyses of stochastic trial-by-trial variation in skin displacement further confirmed the link between the differences in the size of the partial slip area and subjects' judgement of differences in slipperiness.

The largest fraction of the skin slipping over the surface comprised net unilinear displacement. Other patterns of skin displacement such as the displacement jitter and divergence comprised only a minor fraction. The magnitude of skin displacement associated with the divergence was dependent on friction. Importantly, with the natural reach and touch movement, the constraints applied to the arm movement kinematics significantly reduced the divergence to one-third of what it was with the natural reach and touch movement.

Thus, natural reaching movement kinematics profoundly enhanced the availability of friction-related sensory cues related to the divergence pattern. This is because the lateral movement promoting partial slips facilitated the release of stress in radial patterns as predicted by the skin mechanical modelling (Willemet et al., 2021). Because the magnitude of unilinear skin displacement concurrently caused profoundly larger divergence magnitudes, the relative significance of the two in signalling friction currently cannot be separated. It could be speculated that the ratio between the unilateral displacement and divergence might be exploited to reduce ambiguity in extracting frictional information from the amount of skin displacement, as a result of the stochastic size of tangential movement. For example, in situations when greater lateral forces cause a relatively large net, skin displacement occurs on a less slippery surface than with a more slippery surface. One alternative possibility to reduce ambiguity of contact forces and skin displacement in a real-life situation requires combining the magnitude of skin displacement with information about the skin stretch pattern caused by the lateral movement (Ingvars et al., 2001, 2009; Seizova-Cajic et al., 2014) or torsion in the finger pad (du Bois de Dunilac et al., 2023; Khamis et al., 2015; Loutit et al., 2023). As in virtual environments, tangential skin stretches within the contact area ranging between 0.25 and 0.75 mm lead to friction perception (Kamikawa & Okamura, 2018; Provancher & Sylvester, 2009; Santello et al., 2002; Suchoski et al., 2018).

The present study has identified the neurophysiological role of active movement kinematics in how frictional information is obtained and used by the brain for perception. This shows for the first time that small lateral movements as a part of natural motor control during grasping help to inform our perception of friction between the finger pad skin and the object being touched. Our findings can inform engineers of how programmed movement tremor may improve the sensitivity of tactile sensors (Huloux et al., 2021; Khamis et al., 2019, 2021), which could measure friction (Chen et al., 2018; Khamis et al., 2018; Ulloa et al., 2022), as well as help in the design of tactile displays that make use of friction modulation principles (Gueorguiev et al., 2017; Vardar et al., 2017). The present study also has implications for the design of neural prostheses and extends the understanding of the tactile sensorimotor control strategies required for dexterous object manipulation (Bensmaia et al., 2023; Suresh et al., 2020).

References

Afzal, N., Stubbs, E., Khamis, H., Loutit, A. J., Redmond, S. J., Vickery, R. M., Wiertlewski, M., & Birznieks, I. (2022). Submillimeter lateral displacement enables friction sensing and awareness of surface slipperiness. *Institute of Electrical and Electronics Engineers Transactions on Haptics*, **15**(1), 20–25.

Barrea, A., Delhaye, B. P., Lefèvre, P., & Thonnard, J.-L. (2018). Perception of partial slips under tangential loading of the fingertip. *Scientific Reports*, **8**(1), 7032.

Bensmaia, S. J., Tyler, D. J., & Micera, S. (2023). Restoration of sensory information via bionic hands. *Nature Biomedical Engineering*, **7**(4), 443–455.

Birznieks, I., Burstedt, M. K. O., Edin, B. B., & Johansson, R. S. (1998). Mechanisms for force adjustments to unpredictable frictional changes at individual digits during two-fingered manipulation. *Journal of Neurophysiology*, **80**(4), 1989–2002.

Chen, W., Khamis, H., Birznieks, I., Lepora, N. F., & Redmond, S. J. (2018). Tactile sensors for friction estimation and incipient slip detection—toward dexterous robotic manipulation: A review. *Institute of Electrical and Electronics Engineers Sensors Journal*, **18**(22), 9049–9064.

Delhaye, B., Barrea, A., Edin, B. B., Lefèvre, P., & Thonnard, J. L. (2016). Surface strain measurements of fingertip skin under shearing. *Journal of The Royal Society Interface*, **13**(115), 20150874.

Delhaye, B., Lefèvre, P., & Thonnard, J. L. (2014). Dynamics of fingertip contact during the onset of tangential slip. *Journal of The Royal Society Interface*, **11**(100), 20140698.

du Bois de Dunilac, S., Córdova Bulens, D., Lefèvre, P., Redmond, S. J., & Delhaye, B. P. (2023). Biomechanics of the finger pad in response to torsion. *Journal of The Royal Society Interface*, **20**(201), 20220809.

Gueorguiev, D., Vezzoli, E., Mouraux, A., Lemaire-Semail, B., & Thonnard, J.-L. (2017). The tactile perception of transient changes in friction. *Journal of The Royal Society Interface*, **14**(137), 20170641.

Huloux, N., Bernard, C., & Wiertlewski, M. (2021). Estimating friction modulation from the ultrasonic mechanical impedance. *Institute of Electrical and Electronics Engineers Transactions on Haptics*, **14**(2), 409–420.

Ingvars, B., Per, J., Antony, W. G., & Roland, S. J. (2001). Encoding of direction of fingertip forces by human tactile afferents. *The Journal of Neuroscience*, **21**(20), 8222–8237.

Ingvars, B., Vaughan, G. M., Göran, W., & Roland, S. J. (2009). Slowly adapting mechanoreceptors in the borders of the human fingernail encode fingertip forces. *The Journal of Neuroscience*, **29**(29), 9370–9379.

Johansson, R. S., & Flanagan, J. R. (2009). Coding and use of tactile signals from the fingertips in object manipulation tasks. *Nature Reviews Neuroscience*, **10**(5), 345–359.

Johansson, R. S., & Westling, G. (1987). Signals in tactile afferents from the fingers eliciting adaptive motor responses during precision grip. *Experimental Brain Research*, **66**(1), 141–154.

Kamikawa, Y., & Okamura, A. (2018). Comparison between force-controlled skin deformation feedback and hand-grounded kinesthetic force feedback for sensory substitution. *Institute of Electrical and Electronics Engineers Robotics and Automation Letters*, **3**(3), 2174–2181.

Khamis, H., Afzal, H. M. N., Sanchez, J., Vickery, R., Wiertlewski, M., Redmond, S. J., & Birznieks, I. (2021). Friction sensing mechanisms for perception and motor control: Passive touch without sliding may not provide perceivable frictional information. *Journal of Neurophysiology*, **125**(3), 809–823.

Khamis, H., Benjamin, X., Redmond, S. J., & Redmond, S. J. (2019). A novel optical 3D force and displacement sensor – Towards instrumenting the PapillArray tactile sensor. *Sensors and Actuators A: Physical*, **291**, 174–187.

Khamis, H., Birznieks, I., & Redmond, S. J. (2015). Decoding tactile afferent activity to obtain an estimate of instantaneous force and torque applied to the fingerpad. *Journal of Neurophysiology*, **114**(1), 474–484.

Khamis, H., Izquierdo Albero, R., Salerno, M., Shah Idil, A., Loizou, A., & Redmond, S. J. (2018). PapillArray: An incipient slip sensor for dexterous robotic or prosthetic manipulation – design and prototype validation. *Sensors and Actuators A: Physical*, **270**, 195–204.

Khamis, H., Redmond, S. J., Macefield, V., & Birznieks, I. (2014a). Classification of texture and frictional condition at initial contact by tactile afferent responses. In M. Auvray, & C. Duriez (Eds.), *Haptics: Neuroscience, Devices, Modeling, and Applications* (pp. 460–468). Springer Berlin Heidelberg.

Khamis, H. A., Redmond, S. J., Macefield, V. G., & Birznieks, I. (2014b). Tactile afferents encode grip safety before slip for different frictions. In *2014 36th Annual International Conference of the IEEE Engineering in Medicine and Biology Society* (pp. 4123–4126). IEEE.

Loutit, A. J., Wheat, H. E., Khamis, H., Vickery, R. M., Macefield, V. G., & Birznieks, I. (2023). How tactile afferents in the human fingerpad encode tangential torques associated with manipulation: Are monkeys better than us? *The Journal of Neuroscience*, **43**(22), 4033–4046.

Lucas, B. D., & Kanade, T. (1981). An Iterative Image Registration Technique with an Application to Stereo Vision (IJCAI), vol. **2**. In *Proceedings of the 7th international joint conference on Artificial intelligence*, Vancouver, BC, Canada.

Provancher, W. R., & Sylvester, N. D. (2009). Fingerpad skin stretch increases the perception of virtual friction. *Institute of Electrical and Electronics Engineers Transactions on Haptics*, **2**(4), 212–223.

Santello, M., Martha, F., & John, F. S. (2002). Patterns of hand motion during grasping and the influence of sensory guidance. *The Journal of Neuroscience*, **22**(4), 1426–1435.

Seizova-Cajic, T., Karlsson, K., Bergstrom, S., McIntyre, S., & Birznieks, I. (2014). Lateral Skin Stretch Influences Direction Judgments of Motion Across the Skin. In M. Auvray, & C. Duriez (Eds.), *Haptics: Neuroscience, Devices, Modeling, and Applications* (pp. 425–431). Springer Berlin Heidelberg.

Shi, J., & Tomasi, C. (1994). Good features to track. In *1994 Proceedings of IEEE conference on computer vision and pattern recognition* (pp. 593–600).

Suchoski, J. M., Martinez, S. J., & Okamura, A. M. (2018). Scaling inertial forces to alter weight perception in virtual reality. *IEEE International Conference on Robotics and Automation* (pp. 484–489).

Suresh, A. K., Goodman, J. M., Okorokova, E. V., Kaufman, M., Hatsopoulos, N. G., & Bensmaia, S. J. (2020). Neural population dynamics in motor cortex are different for reach and grasp. *Elife*, **9**, e58848.

Tada, M., & Kanade, T. (2004). An imaging system of incipient slip for modelling how human perceives slip of a fingertip. In *The 26th Annual International Conference of the Institute of Electrical and Electronics Engineers Engineering in Medicine and Biology Society*, **2004**, 2045–2048.

Tomasi, C., & Kanade, T. (1991). Detection and tracking of point. *International Journal of Computer Vision*, **9**, 3.

Ulloa, P. M., Bulens, D. C., & Redmond, S. J. (2022). Incipient slip detection for rectilinear movements using the papillarray tactile sensor. *2022 Institute of Electrical and Electronics Engineers Sensors*, 1–4.

Vardar, Y., Guclu, B., & Basdogan, C. (2017). Effect of waveform on tactile perception by electrovibration displayed on touch screens. *Institute of Electrical and Electronics Engineers Transactions on Haptics*, **10**(4), 488–499.

Wiertlewski, M., Fenton Friesen, R., & Colgate, J. E. (2016). Partial squeeze film levitation modulates fingertip friction. *Proceedings of the National Academy of Sciences*, **113**(33), 9210–9215.

Willemet, L., Kanzari, K., Monnoyer, J., Birznieks, I., & Wiertlewski, M. (2021). Initial contact shapes the perception of friction. *Proceedings of the National Academy of Sciences*, **118**(49), e2109109118.

Zhou, X., Li, Y., Tian, Y., Masen, M. A., Li, Y., & Jin, Z. (2023). Friction and neuroimaging of active and passive tactile touch. *Scientific Reports*, **13**(1), 13077.

Additional information

Data availability statement

Data could be obtained from the authors upon reasonable request.

Competing interests

The authors declare that they have no competing interests.

Author contributions

N.A. developed the setup, conducted the experiments, analysed the data and drafted/revised the work. S.B.D., P.M.U., H.O.S. and A.J.L. processed the images, developed the algorithm for feature extraction and extracted the data. IB, RV, SJ and MW contributed to the conception of the work and revised the manuscript critically for important intellectual content. HK and NA conceptualised and designed the work, analysed and interpreted data, and drafted/revised the work. All authors approved the final version of the manuscript submitted for publication. All authors agree to be accountable for all aspects of the work in ensuring that questions related to the accuracy or integrity of any part of the work are appropriately investigated and resolved. All persons designated as authors qualify for authorship and all those who qualify for authorship are listed.

Funding

This project was funded by the Australian Research Council Discovery Grants DP230100048 and DP200100630.

Acknowledgements

We thank Mr Hilary Carter (NeuRA) for assistance with mechanical works.

Open access publishing facilitated by University of New South Wales, as part of the Wiley - University of New South Wales agreement via the Council of Australian University Librarians.

Keywords

force control, friction, hand, manipulation, motor control, perception, slip, tactile

Supporting information

Additional supporting information can be found online in the Supporting Information section at the end of the HTML view of the article. Supporting information files available:

Peer Review History